NATIONAL ADVISORY COMMITTEE FOR AERONAUTICS

TECHNICAL NOTE 1921

APPROXIMATE METHOD FOR PREDICTING FORM AND LOCATION OF DETACHED SHOCK WAVES AHEAD OF PLANE OR AXIALLY SYMMETRIC BODIES

By W. E. Moeckel

Lewis Flight Propulsion Laboratory
Cleveland, Ohio

NACA

Washington
July 1949

NATIONAL ADVISORY COMMITTEE FOR AERONAUTICS

TECHNICAL NOTE 1921

APPROXIMATE METHOD FOR PREDICTING FORM AND LOCATION OF DETACHED SHOCK WAVES AHEAD OF PLANE OR AXIALLY SYMMETRIC BODIES

By W. E. Moeckel

SUMMARY

An approximate method, based on a simplified form of the continuity relation, is developed to predict the location of detached shock waves ahead of two-dimensional and axially symmetric bodies. In order to reduce the problem to an equivalent one-dimensional form, it was assumed that: (1) The form of the shock between its foremost point and its sonic point is adequately represented by an hyperbola asymptotic to the free-stream Mach lines; and (2) the sonic line between the shock and the body is straight and inclined at an angle that depends only on the free-stream Mach number. With these assumptions, the location of the shock relative to the body sonic point is independent of the form of the nose or leading edge ahead of the sonic point and becomes a single-valued function of the Mach number. A simple geometric method for estimating shock location is also presented, but this method agrees less closely with experiment than the continuity method.

When the location of the detached wave and the sonic line relative to the body are known, the drag of the portion of the body upstream of its sonic point can be estimated from the momentum change of the fluid that crosses the sonic line. Comparison with available experimental results indicates that the estimated drag coefficients are good approximations except for very blunt bodies and for free-stream Mach numbers close to 1.0.

The simplified continuity method is also applied to unsymmetric two-dimensional bodies at angle of attack and to two-dimensional and axially symmetric supersonic inlets with detached waves due to spillage over the cowl. For supersonic inlets, the relation between spillage and shock location is presented and the additive drag due to spillage is estimated.

INTRODUCTION

When a region of subsonic flow occurs in a supersonic flow field, many simplifying assumptions are generally required to make theoretical analysis feasible. Without such assumptions, the flow can be constructed only by means of lengthy numerical methods based on differential equations of fluid mechanics. Such computations differ for each configuration investigated; general trends and important parameters are therefore not easily discernible.

A reasonable set of assumptions for simplifying the analysis of supersonic flow with detached shock waves should be consistent with the following characteristics of such flow fields: The entropy varies from the free-stream value to the value behind a normal shock, and the velocity varies from the free-stream value to zero at the stagnation point. Thus, if the free-stream Mach number is considerably greater than unity and if the subsonic region is a significant part of the entire disturbed flow field, analyses based on such assumptions as irrotational flow, small differences between local and free-stream velocity, or incompressible flow in the subsonic region can no longer be expected to yield valid results. For such problems, other simplifying assumptions must therefore be formulated.

An analysis based on assumptions concerning the form of the boundaries of the subsonic region rather than on the nature of the flow variables is presented herein. In this analysis, which was made at the NACA Lewis laboratory, both plane and axially symmetric bodies were considered. The form of the detached wave is assumed to be only secondarily influenced by the form of the body ahead of the sonic point, and the sonic line between the shock and the body is assumed to be straight and inclined at an angle that depends only on the free-stream Mach number. The continuity relation is then applied to this simplified picture to obtain the location of the shock relative to the sonic point for plane and axially symmetric bodies. The drag is estimated from the momentum change of the fluid that passes the sonic line. The method is also applied to plane unsymmetric bodies at angle of attack and to two-dimensional and axially symmetric supersonic inlets with spillage over the cowl. Results are compared, where possible, with available experimental data.

SYMBOLS

The following symbols are used, some of which are illustrated in figure 1:

A area

a speed of sound

$B = \sigma\left(\frac{P_0}{P_s}\right)_\sigma$

b x-coordinate of foremost point of body

$C \quad \beta\left(\beta \tan \varphi_s - \sqrt{\beta^2 \tan^2 \varphi_s - 1}\right)$

C_D drag coefficient of portion of body ahead of theoretical sonic point (based on area indicated by subscript)

$k = \frac{1}{\gamma M_0^2}\left[1.2679\left(\frac{P_s}{P_0}\right)_\sigma \frac{P_0}{p_0} - 1\right]$

L distance between vertex of detached shock wave and x_{BB}

M free-stream Mach number

P stagnation pressure

p static pressure

V local velocity

x coordinate in stream direction

x_0 distance from foremost point of detached shock to intercept of its asymptote on x-axis

y coordinate perpendicular to stream direction

$\beta \quad \sqrt{M^2 - 1}$

γ ratio of specific heats (1.4 for air)

δ local angle of body contour relative to x-axis

η angle between sonic line and normal to free-stream direction

θ half-angle of wedge or cone

θ_d cone half-angle for which shock becomes detached

λ angle of streamline relative to x-axis

λ_d wedge half-angle for which shock becomes detached

ρ density

σ isentropic contraction ratio from free stream to sonic velocity

τ fraction of maximum possible inlet mass flow that passes outside cowl

φ local inclination of detached shock relative to x-axis

Subscripts:

0 free-stream conditions

1,2 upper and lower portion of unsymmetric body contour, respectively

c centroid of stream tube passing sonic line

cr critical conditions

S sonic point of detached shock

SB sonic point of body

s conditions along sonic line

ANALYSIS

The representation of flow with detached shock waves to be used in the present analysis is shown in figure 1. The region of subsonic flow is bounded by the portion of the detached wave below its sonic point S, by the portion of the body contour upstream of its sonic point SB, and by the sonic curve between S and SB. If the form of the detached wave is known, the location of S on the shock can immediately be determined, because for a given M_0 the angle φ_S for which sonic velocity exists behind the shock is known from shock theory. The flow direction λ_S at this point is then also known.

The sonic curve is shown in figure 1 as a straight line. This approximation is used throughout the analysis, although more exact computations, as well as experimental results, indicate that the form may depend considerably on the shape of the nose or leading edge (references 1 and 2). To the degree of approximation of the present method, however, such variations appear to be unimportant. With the simplified picture shown in figure 1, approximate expressions can be derived for the shock location relative to the body sonic point and for the drag of the portion of the body in the subsonic-flow region.

Location of Body Sonic Point

Evidence is available to show that, for bodies with sharp or well-defined shoulders (fig. 2(a)), the sonic point is located at the shoulder (reference 2). For more gradually curved bodies, such as ogives, the location of the sonic point can be estimated by an extension of a method suggested by Busemann (reference 3). This method locates the shoulder at the point where the contour of the body is inclined at the wedge angle or cone angle corresponding to shock detachment (fig. 2(b)). If the sonic line is approximated by a straight line, the location of the shoulder and the sonic point coincide. These results are analogous, in some ways, with the flow past the throat section of a supersonic nozzle, for which the location of the maximum constriction (shoulder) and the sonic point coincide if the throat is sharp or if the flow is treated as one dimensional.

The choice of the point of tangency of the body with a line inclined at the detachment angle as the approximate location of the sonic point has some theoretical justification for two-dimensional flow. W. Perl has pointed out to the author that for flow near sonic velocity and for small perturbation velocities, the derivative $\partial\lambda/\partial\nu$ taken along the normal to a streamline, vanishes to a first approximation at the intersection of the sonic line with the shock wave. This result implies that λ is relatively constant along the sonic line and hence, that the inclination of the body at its sonic point is approximately equal to λ_S. Inasmuch as λ_S

is slightly smaller than λ_d, the sonic point would be located slightly downstream of the shoulder of the body; whereas the discussion given in reference 3 shows that the sonic point lies ahead of the shoulder. These differences, however, are insignificant for the present analysis, because the sonic point and the shoulder are assumed to coincide.

Although the theoretical basis for locating the sonic point by means of the detachment angle is far from complete, particularly for axially symmetric bodies, the procedure appears reasonable if, as assumed in the present analysis, the form of the nose or leading edge ahead of the shoulder (or sonic point) has only a secondary effect on the form and the location of the sonic line. This sonic line should therefore have almost the same form for all bodies as, for example, for a wedge or a cone with half-angle only slightly greater than the detachment angle. Because the sonic point for these bodies is known to be located at the point of tangency with the detachment angle, the procedure should be valid for all bodies at the same Mach number within the degree of approximation of the present method. This procedure will therefore be used to determine body sonic points for comparison of theoretical and experimental results.

The reasoning used in the preceding paragraph leads to a very simple geometric method for predicting the location of detached shock waves. A wedge or a cone with included angle large enough to cause shock detachment and with well-defined shoulders is considered (fig. 2(a)). If $b-x_0$ is the distance from the vertex of the cone or wedge to the foremost point of the detached wave, then

$$\frac{b-x_0}{y_{SB}} = \frac{L}{y_{SB}} - \cot \theta \tag{1}$$

If θ is now set equal to the detachment angle, then $b-x_0$ becomes zero, and the expressions for shock location become:

for plane flow,

$$\frac{L}{y_{SB}} = \cot \lambda_d \tag{2}$$

and for axially symmetric flow,

$$\frac{L}{y_{SB}} = \cot \theta_d \tag{3}$$

Because, by the present assumptions, L/y_{SB} is constant for a given M_0 and independent of the form of the nose, equations (2) and (3) represent estimates of the location of the detached shock wave for all bodies at zero angle of attack. This estimate should be particularly valid for bodies only slightly blunter than the wedge or cone for which detachment occurs. The following derivation, however, which is based on the continuity relation, should provide a better estimate of the average shock location for more general blunt bodies.

1142

Location of Detached Shock Wave (Continuity Method)

Assumed form of detached shock wave. - The most typical characteristics of detached waves are that: (1) They are normal to the free stream at their foremost point; and (2) they are asymptotic to the free-stream Mach lines at large distances from their foremost point. A simple curve that has these characteristics is an hyperbola represented by

$$\beta y = \sqrt{x^2 - x_0^2} \tag{4}$$

where β is the cotangent of the Mach angle and x_0 is the distance from the vertex of the wave to the intersection of its asymptotes. For the purpose of the analysis, the hypothesis is made that to the degree of approximation required, all detached waves in the region between the axis and the sonic point S may be represented by equation (4).

With this form of detached wave, the angle between the stream direction and the tangent to the shock at any point is obtained from (fig. 1)

$$\frac{dy}{dx} = \tan \varphi = \frac{x}{\beta \sqrt{x^2 - x_0^2}} = \frac{\sqrt{x_0^2 + \beta^2 y^2}}{\beta^2 y} \tag{5}$$

The location of S is then

$$y_S = \frac{x_0 \cot \varphi_S}{\beta\sqrt{\beta^2 - \cot^2 \varphi_S}} \tag{6}$$

$$x_S = \frac{\beta x_0}{\sqrt{\beta^2 - \cot^2 \varphi_S}} \tag{6a}$$

If the y-coordinate of the body sonic point is used as the reference dimension, then the form of the shock wave is given by (equation (4))

$$\frac{y}{y_{SB}} = \frac{1}{\beta}\sqrt{\left(\frac{x}{y_{SB}}\right)^2 - \left(\frac{x_0}{y_{SB}}\right)^2} \tag{7}$$

where, from equation (6),

$$\frac{x_0}{y_{SB}} = \beta \frac{y_S}{y_{SB}}\sqrt{\beta^2 \tan^2 \varphi_S - 1} \tag{8}$$

From equation (6a) the dimensionless location of the shock sonic point is

$$\frac{x_S}{y_{SB}} = \frac{\beta \frac{x_0}{y_{SB}}}{\sqrt{\beta^2 - \cot^2 \varphi_S}} \tag{9}$$

The distance from the foremost point of the shock to the x-coordinate of the body sonic point is

$$\frac{L}{y_{SB}} = \frac{x_{SB}}{y_{SB}} - \frac{x_0}{y_{SB}} \tag{10}$$

where, from figure 1,

$$\frac{x_{SB}}{y_{SB}} = \frac{x_S}{y_{SB}} + \left(\frac{y_S}{y_{SB}} - 1\right) \tan \eta \tag{11}$$

If equations (8), (9), and (11) are combined to eliminate all unknown coordinates except y_S and L, equation (10) becomes

$$\frac{L}{y_{SB}} = \frac{y_S}{y_{SB}}(C + \tan \eta) - \tan \eta \tag{12}$$

where

$$C = \beta\left(\beta \tan \varphi_S - \sqrt{\beta^2 \tan^2 \varphi_S - 1}\right) \tag{13}$$

Inasmuch as β and φ_S are known for any given free-stream Mach number, only the quantities y_S/y_{SB} and η remain to be determined to predict the relation between the sonic point on a body and the location of its detached wave.

Application of continuity equation. - In order to determine the quantity y_S/y_{SB}, the continuity relation is applied to the fluid that passes the sonic line. The integral form of this relation is useless for the present method, inasmuch as the distribution of the flow variables along the sonic line is unknown. The distribution of stagnation pressure immediately behind the shock, however, is known. An appropriate average value of this quantity is that existing along the streamline which represents the mass centroid of the fluid passing the sonic line. This centroid streamline enters the shock wave at $y_c = y_S/2$ for plane flow and at $y_c = 2y_S/3$ for axially symmetric flow. The shock angle corresponding to these values of y can be obtained from equations (5) and (6). Because the stagnation pressure remains constant along each streamline behind the shock, the value of $P_{s,c}$ will remain unchanged between the shock wave and the sonic line. Because the total temperature is constant, the simplified continuity equation may be written as

$$\frac{A_0}{A_s} = \frac{(\rho_s V_s)_c}{\rho_0 V_0} = \left(\frac{P_s}{P_0}\right)_c \left[\frac{(\rho V)_{cr}}{\rho_0 V_0}\right] = \left(\frac{P_s}{P_0}\right)_c \frac{1}{\sigma} \tag{14}$$

where σ is the contraction ratio required to decelerate the free stream to sonic velocity isentropically. In terms of the coordinates of the sonic points, equation (14) becomes, for plane flow

$$\frac{y_S - y_{SB}}{\cos \eta} = \left(\frac{P_0}{P_s}\right)_c \sigma y_S = B y_S$$

or

$$\frac{y_S}{y_{SB}} = (1 - B \cos \eta)^{-1} \tag{15}$$

and for axially symmetric flow

$$\frac{y_S^2 - y_{SB}^2}{\cos \eta} = \left(\frac{P_0}{P_s}\right)_c \sigma y_S^2 = B y_S^2$$

or

$$\frac{y_S}{y_{SB}} = (1 - B \cos \eta)^{-\frac{1}{2}} \tag{16}$$

The appropriate values of η to be used in each case remain to be established. On the basis of the previously cited analogy between one-dimensional channel flow and flow with detached shock waves, the sonic line is assumed to be normal to the average flow direction in its vicinity. At S the inclination of the flow is known to be λ_S both for plane and axially symmetric flow; whereas at SB the inclination is assumed to be λ_d for plane flow and θ_d for axially symmetric flow. If the arithmetic mean of the inclinations at the two extremities is used, the appropriate expressions for η become:

for plane flow,

$$\eta = \tfrac{1}{2}(\lambda_d + \lambda_S) \tag{17}$$

and for axially symmetric flow,

$$\eta = \tfrac{1}{2}(\theta_d + \lambda_S) \tag{18}$$

Because λ_S differs only slightly from λ_d, the inclination of the sonic line for plane flow will be assumed to be simply $\eta = \lambda_S$. Values of y_S/y_{SB} obtained from equations (15) and (16) are shown as functions of M_0 in figure 3. The variation of x_0/y_{SB} with M_0, as computed from equation (8), is also shown. The values of λ_S and θ_d required to determine y_S/y_{SB} were obtained from the shock charts of reference 4 and are plotted against M_0 in figure 4. The shock angle at the sonic point φ_S and the shock angles at the mass centroid for two-dimensional and axially symmetric flow are also shown in figure 4. In figure 5, the resulting total-pressure ratios $(P_s/P_0)_c$ are given together with the values of σ and C used in equations (13) through (16).

Comparison of Theoretical and Experimental Shock Location

A comparison of the shock form and location estimated by the continuity method with the experimental results of reference 2 is shown in figure 6. The data of reference 2 were obtained with a free jet with an outlet Mach number of 1.7. The flow field in the vicinity of the models was reconstructed from interferograms. For comparison of theory and experiment, the foremost point of the detached wave was used as the common point. The theoretical configuration is independent of the body form and is therefore the same for each of the three bodies shown. For the sphere and the cone, experimental sonic points are given in reference 2 and the y-coordinate of these points was used as the reference dimension. For the projectile, however, the actual sonic point was not determined in reference 2 and the theoretically estimated location of this point was used as the reference dimension. The assumed shock form and the estimated distance from the vertex of the shock to the body sonic point are shown to be approximately in agreement with

experimental results for all three bodies. Increasing bluntness of the nose appears to shift the upper portion of the detached wave away from the body, but in view of the wide range of nose forms this effect appears to be small. The shock form for the projectile may be somewhat in error in figure 6 due to the relatively small scale of the subsonic portion of the diagram presented for this body (reference 2).

The theoretical variation of L/y_{SB} with Mach number is shown in figure 7 for plane and axially symmetric bodies, together with available experimental values from references 1, 5, and 6, and the numerically computed values of reference 1. The data obtained from reference 6 were converted to the present parameters from a small sketch of the model and may therefore be somewhat in error. The values obtained by the continuity method are seen to agree more closely, in general, with experimental results than the values obtained by the geometric method. As previously stated, however, the geometric method should yield more accurate results for bodies only slightly blunter than the wedge or cone for which shock detachment occurs. This prediction is born out to some extent for the two-dimensional bodies, where the value obtained in reference 1 for the wedge agrees closely with the value obtained by the geometric method, and the continuity method appears to average the results obtained for the wedge and the flat-nosed body. For the axially symmetric bodies no such comparison is available, although figure 6 shows that L/y_{SB} tends to increase as the body becomes less blunt. These results indicate that the continuity method leads to an average value of L/y_{SB}; whereas the geometric method yields the maximum value of this quantity for a given M_0.

Drag Upstream of SB

Because the form and the location of the shock wave and the sonic line are assumed to be independent of the shape of the nose or the leading edge, it follows that the drag coefficient of the portion of the body upstream of its sonic point is, by the present method, also independent of the body form. This portion of the drag can be determined from the momentum theorem. If the streamlines are assumed to be normal to the sonic line and if average values of the flow variables at the sonic line are again used, the momentum equation may be written as (fig. 1)

$$\int_b^{SB} (p-p_0)dA \sin\delta = \rho_0 V_0^2 A_0 - (\rho_s V_s^2)_c A_s \cos\eta - (p_{s,c}-p_0)A_s \cos\eta \tag{19}$$

1142

from which the drag coefficient based on A_0 becomes

$$(C_D)_{A_0} = \frac{\int_b^{SB} (p-p_0)dA \sin\delta}{\frac{1}{2}\rho_0 V_0^2 A_0}$$

$$= 2\left\{1 - \left[\frac{(\rho_s V_s^2)_c}{\rho_0 V_0^2} + \frac{\left(\frac{p_s}{p_0}\right)_c - 1}{\gamma M_0^2}\right]\frac{A_s}{A_0}\cos\eta\right\}$$

$$= 2\left\{1 + \frac{A_s}{A_0}\frac{\cos\eta}{\gamma M_0^2}\left[1 - (\gamma+1)\left(\frac{p_s}{p_0}\right)_c\right]\right\} \tag{20}$$

Using the value of A_s/A_0 from equation (14), equation (20) becomes

$$(C_D)_{A_0} = 2\left\{1 + \frac{\sigma\cos\eta}{\gamma\frac{p_0}{p_0}M_0^2}\left[\frac{p_0}{p_0}\left(\frac{p_0}{p_s}\right)_c - \frac{p_s}{p_s}(\gamma+1)\right]\right\} \tag{21}$$

where $\frac{p_s}{p_s} = 0.5283$.

The drag coefficient based on the area of the body at its sonic point is:

for plane flow,

$$(C_D)_{A_{SB}} = (C_D)_{A_0}\left(\frac{y_S}{y_{SB}}\right) \tag{22}$$

and for axially symmetric flow,

$$(C_D)_{A_{SB}} = (C_D)_{A_0}\left(\frac{y_S}{y_{SB}}\right)^2 \tag{23}$$

If the appropriate values of η, $(P_s/P_0)_c$, and y_S/y_{SB} are used, the expressions for the drag coefficient become idential for plane and axially symmetric flow:

$$(C_D)_{A_{SB}} = 2\left(\frac{1 - kB\cos\eta}{1 - B\cos\eta}\right) \tag{24}$$

where

$$k = \frac{1}{\gamma M_0^2}\left[1.2679\left(\frac{P_s}{P_0}\right)_c\frac{P_0}{p_0} - 1\right] \tag{25}$$

These drag coefficients are plotted against M_0 in figure 8, together with the experimental values obtained from reference 2 by numerical integration of the pressure coefficients given therein and the theoretical values for flat-nosed bodies and for a wedge computed in reference 1. The theoretical values obtained by the present method are not expected to be valid near $M_0 = 1.0$, because the subsonic field becomes very large relative to the body ($y_S/y_{SB} \longrightarrow \infty$) and small variations in the assumed form and inclination of the sonic line have a large effect on the computed drag. Equation (24) becomes indeterminate for $M_0 = 1$ because $\cos\eta$, B, and k are all unity for sonic free-stream velocity.

The agreement with experimental data for the cone and the sphere at $M_0 = 1.7$ is seen to be good. The drag coefficients computed for the flat-nosed bodies in reference 1, however, fall considerably above the values obtained by the present method. Part of this disagreement is probably due to the somewhat extreme form of the

sonic line assumed for these bodies in the computations of reference 1. This assumed sonic line meets the face of the body perpendicularly at the shoulder, whereas the actual sonic line is probably concave downstream. (See fig. 6.) Some disagreement should probably be expected, however, inasmuch as the momentum integral used to obtain the drag coefficient by the present method is more sensitive to differences in the stream angle near the sonic line than the continuity equation used to predict shock location. The present procedure is therefore most valid when the streamlines are expected to be almost normal to the sonic line and when the sonic line is not expected to have large curvature.

The maximum possible drag coefficient, obtained by assuming that the stagnation pressure behind a normal shock acts on the entire nose, is plotted in figure 8 for comparison.

Unsymmetric Bodies and Effect of Angle of Attack for Two-Dimensional Flow

If the method used for determining the location of SB for symmetric bodies is applied to unsymmetric bodies or to bodies at angle of attack, the magnitude of the coordinates of the upper and lower sonic points will, in general, differ (fig. 9). It is apparent that portions of figure 9 above and below the center line between the two tangent lines are each similar to the configuration shown in figure 2(b). Such a representation, however, can be considered valid only for bodies that can be completely described in two dimensions. If the reasoning used to locate the sonic point for symmetric bodies at zero incidence is followed, then variations of the portion of the body between SB,1 and SB,2 will not appreciably alter the location of the sonic points or the form and the location of the detached wave and the sonic line. The continuity method can be applied separately to the portions of the flow field above and below the zero streamline (that is, the streamline that reaches the stagnation point on the body). The location of this streamline need be known only in the free stream ahead of the detached wave. The assumption that this streamline must pass through the intersection of the two tangent lines (fig. 9) is consistent with the reasoning used to locate the sonic points. Because the upper and lower portions can be treated separately, equations (15) and (16) lead to the result

$$\frac{y_{S,1}}{y_{SB,1}} = \frac{y_{S,2}}{y_{SB,2}} = \frac{y_S}{y_{SB}} \tag{26}$$

Therefore, from equations (8) and (12),

$$\frac{x_{0,1}}{y_{SB,1}} = \frac{x_{0,2}}{y_{SB,2}} = \frac{x_0}{y_{SB}} \tag{27}$$

and

$$\frac{L}{y_{SB,1}} = \frac{L}{y_{SB,2}} = \frac{L}{y_{SB}} \tag{28}$$

The equations for the portions of the shock wave above and below the x-axis are:

Upper

$$\frac{\beta y}{y_{SB,1}} = \sqrt{\left(\frac{x}{y_{SB,1}}\right)^2 - \left(\frac{x_0}{y_{SB}}\right)^2} \tag{29}$$

Lower

$$\frac{\beta y}{y_{SB,2}} = \sqrt{\left(\frac{x}{y_{SB,2}}\right)^2 - \left(\frac{x_0}{y_{SB}}\right)^2} \tag{29a}$$

An example of the resulting configuration for an unsymmetric two-dimensional body is shown in figure 10 for $y_{SB,2} = 0.5y_{SB,1}$. The values of y_S/y_{SB} and x_0/y_{SB} were obtained from figure 3 and L/y_{SB} was obtained from the results of the continuity method (fig. 7). A slight discrepancy appears in the location of the vertex of the detached wave due to the separate construction of the upper and lower portions of the configuration, but this discrepancy is well within the accuracy of the approximations. Use of the geometric method would locate the origin of the shock at the point of intersection of the tangent lines from the sonic points. This method would avoid the discontinuity at the vertex of the shock, but would fail to satisfy the continuity equation.

From equations (21) and (22), the drag coefficient of the lower and upper portions of the body are seen to be dependent, for a given M_0, only on y_S/y_{SB}, so that the drag coefficient for the

portion of the unsymmetric body ahead of the sonic points based on $(y_{SB,1} + y_{SB,2})$ is identical to the drag coefficient based on A_{SB} for the symmetric body at zero angle of attack. This result is also evident from the consideration that the momentum change of the fluid that passes the sonic line depends only on the Mach number of the free stream. The total mass flow past the sonic lines depends only on A_{SB}, but the portions of this mass flow above and below the zero streamline are not equal for unsymmetric bodies or for bodies at angle of attack.

In addition to the limitations mentioned in connection with the estimated drag coefficients at zero angle of attack, the fact that regions of negative pressure coefficient may occur when the stagnation streamline fails to intersect the foremost point of the body must also be considered. The drag coefficients estimated by the present method correspond to the integral of the pressure forces over the zero streamline and are independent of the shape of this streamline ahead of the sonic point. Local separation regions near the foremost edge, however, may alter the subsonic portion of the flow sufficiently to invalidate estimates of drag based on a prescribed form of the sonic line and an assumed flow direction. The procedure for estimating the location of the shock, however, should not be greatly in error, because the continuity relation used to predict this location is relatively insensitive to variations in the form of the sonic line or the inclination of the velocity vector.

Shock Location and Additive Drag for Supersonic Inlets with Spillage over Cowl

The method of the preceding sections may be easily extended to the problem of estimating the shock location and the additive drag as functions of the fraction of the maximum mass flow that is spilled over the cowl of two-dimensional or axially symmetric inlets. The simplified picture corresponding to this problem is shown in figure 11, where the y-coordinate is now measured from the axis of symmetry of the inlet. The coordinate y_m denotes the free-stream location of the streamline that separates the mass entering the inlet from that passing outside the inlet. The intersection of this streamline with the detached shock wave is assumed to be the origin of the hyperbolic portion of that shock wave. In terms of the coordinates shown in figure 11, the spillage τ is defined by the following expressions:

Two-dimensional inlets

$$\tau = 1 - \frac{y_m}{y_{SB}} \tag{30}$$

Axially symmetric inlets

$$\tau = 1 - \left(\frac{y_m}{y_{SB}}\right)^2 \tag{30a}$$

The drag due to spillage is defined as the integral of $(p-p_0)$ along the streamline that bounds the entering fluid. This drag is similar to the additive drag defined by Ferri for nose inlets with projecting central bodies, for which the streamlines may be deflected a considerable distance ahead of the cowl.

The sonic point SB can be estimated by the procedure used for closed bodies. For most cases of interest, the lip of the cowl will be sharp or very thin relative to the inlet cross section, so that SB will be very close to the foremost point of the lip. Here the flow rapidly expands to supersonic velocities. Separation regions resulting from this expansion are again neglected and may considerably reduce the additive drag due to spillage. The relation to be derived between spillage and shock location, however, should not be greatly affected by local separation regions.

Other complications usually encountered with supersonic inlets have also been ignored. Oblique shocks from a protruding central body, for example, are assumed to have negligible effect on the relation between mass-flow spillage and drag and on the form of the shock wave above y_m. These simplifications should yield valid estimates when open-nosed bodies without central bodies are considered or when the effect of the central body is felt only below the origin of the hyperbolic portion of the detached shock. The analysis is independent of the nature of the shock below this origin.

The hyperbolic portion of the shock wave is now represented by the equation

$$\beta\left(\frac{y}{y_{SB}} - \frac{y_m}{y_{SB}}\right) = \sqrt{\left(\frac{x}{y_{SB}}\right)^2 - \left(\frac{x_0}{y_{SB}}\right)^2} \tag{31}$$

where

$$\frac{x_0}{y_{SB}} = \beta\sqrt{\beta^2 \tan^2 \varphi_S - 1}\left(\frac{y_S}{y_{SB}} - \frac{y_m}{y_{SB}}\right) \tag{32}$$

Equations (9), (10), and (11) for the x-coordinates of the sonic points and for the shock location remain unchanged by translation of the origin. When equation (32) is used in place of equation (8), the expression for the shock location (equation (10)) becomes

$$\frac{L}{y_{SB}} = \frac{y_S}{y_{SB}}(C + \tan\eta) - C\frac{y_m}{y_{SB}} - \tan\eta \tag{33}$$

Two-dimensional inlets. - For two-dimensional flow, the ratio of the sonic-line flow area to the free-stream area of the stream tube is (fig. 11)

$$\frac{A_S}{A_0} = \frac{y_S - y_{SB}}{(y_S - y_m)\cos\lambda_S} = \left(\frac{p_0}{p_S}\right)_c = B \tag{34}$$

so that

$$\frac{y_S}{y_{SB}} = \frac{1 - \frac{y_m}{y_{SB}} B\cos\lambda_S}{1 - B\cos\lambda_S} \tag{35}$$

If this value is substituted in equation (33), the expression for the location of the vertex of the detached wave becomes

$$\frac{L}{y_{SB}} = \left(1 - \frac{y_m}{y_{SB}}\right)\left(\frac{C + B\sin\lambda_S}{1 - B\cos\lambda_S}\right) \tag{36}$$

When no air passes through the inlet $(y_m = 0)$, this expression is found to reduce to the value obtained for closed symmetric bodies.

The drag coefficient based on A_0 (equation (21)) is independent of the coordinates, so that the drag coefficient for the inlet is obtained by multiplying $(C_D)_{A_0}$ by the ratio A_0/A_{SB}, and becomes

$$(C_D)_{A_{SB}} = (C_D)_{A_0}\left(\frac{y_S}{y_{SB}} - \frac{y_m}{y_{SB}}\right) = (C_D)_{A_0}\left(\frac{y_S}{y_{SB}} - 1 + \tau\right) \qquad (37)$$

Equations (35) and (36) indicate that the distance of the shock from the inlet lip and the drag coefficient for a given M_0 increase linearly with the amount of air that passes outside the inlet.

Axially symmetric inlets. - The ratio of sonic area to free-stream area for axially symmetric inlets becomes

$$\frac{A_s}{A_0} = \frac{y_S^2 - y_{SB}^2}{(y_S^2 - y_m^2)\cos\eta} = B \qquad (38)$$

so that

$$\frac{y_S}{y_{SB}} = \sqrt{\frac{1 - \left(\frac{y_m}{y_{SB}}\right)^2 B\cos\eta}{1 - B\cos\eta}} \qquad (39)$$

For axially symmetric inlets, however, the value of η to be used may be expected to vary with the value of y_m/y_{SB}. When this ratio is close to unity, phenomena near the cowl lip should be almost two dimensional; whereas for large spillage the flow becomes similar to that obtained with closed bodies of revolution. Inasmuch as the cases of relatively small spillage are probably of greater interest, it will be assumed that the flow near the cowl lip is two dimensional so that $\eta = \lambda_S$. Similarly, the two-dimensional value of total-pressure ratio at the mass centroid will be used. By substituting equation (39) into equation (33), the shock location is found to be

$$\frac{L}{y_{SB}} = \sqrt{\frac{1 - \left(\frac{y_m}{y_{SB}}\right)^2 B\cos\lambda_S}{1 - B\cos\lambda_S}}\,(C + \tan\lambda_S) - C\frac{y_m}{y_{SB}} - \tan\lambda_S \qquad (40)$$

Equation (21) for $(C_D)_{A_0}$ may again be multiplied by the ratio A_0/A_{SB} to obtain the drag coefficient based on the inlet area. Thus,

1142

$$(C_D)_{A_{SB}} = (C_D)_{A_0}\left[\left(\frac{y_S}{y_{SB}}\right)^2 - \left(\frac{y_m}{y_{SB}}\right)^2\right] = (C_D)_{A_0}\left[\left(\frac{y_S}{y_{SB}}\right)^2 - 1 + \tau\right] \qquad (41)$$

where η in equation (21) is replaced by λ_S for $y_m \approx y_{SB}$.

The variations of shock location and drag coefficient with τ are shown in figure 12 for two-dimensional and axially symmetric inlets at $M_0 = 2.0$. For axially symmetric inlets, the values obtained using $\eta = \frac{1}{2}(\theta_d + \lambda_S)$ are also plotted for comparison. The value assumed for η evidently has little effect on the estimated drag or the shock location.

SUMMARY OF METHOD

An approximate method has been developed for predicting the location of detached shock waves ahead of plane or axially symmetric bodies and for estimating the drag of the portion of the body upstream of the theoretical sonic point. The method is based on the continuity relation, which is applied to the air that passes the sonic line. The main assumptions were that: (1) The form of the detached wave from the axis to its sonic point is adequately represented by an hyperbola asymptotic to the free-stream Mach lines; and (2) that the sonic curve between the shock and the body is a straight line. These assumptions imply that the form and the location of the shock and the sonic line are only secondarily influenced by the form of the body ahead of its sonic point and that the shock location relative to the body sonic point is primarily a function only of the free-stream Mach number. The drag of the body to the sonic point was estimated from the change of momentum of the air that passes the sonic line and was consequently also independent of the form of the nose or the leading edge in the present approximation.

Comparison with experimental results indicates that the assumptions made are valid to good approximation for predicting the form and the location of detached waves, but may be oversimplifications when it is desired to predict the drag of extremely blunt bodies. The method also fails in the vicinity of sonic free-stream velocity. The effects of angle of attack and unsymmetric body contour are discussed for two-dimensional flow, but no experimental results are available to check the theoretical predictions.

Extension of the method to the problem of estimating the additive drag and the shock location for supersonic inlets with spillage over the cowl indicated that the drag, both for two-dimensional and axially symmetric inlets, increases linearly with the percentage of the maximum inlet mass that passes outside the cowl. The distance between the shock and the inlet lip also increases linearly with this percentage for two-dimensional inlets and almost linearly for axially symmetric inlets.

Lewis Flight Propulsion Laboratory,
National Advisory Committee for Aeronautics,
Cleveland, Ohio, June 1, 1949.

REFERENCES

1. Maccoll, J. W., and Codd, J.: Theoretical Investigations of the Flow around Various Bodies in the Sonic Region of Velocities. Theoretical Res. Rep. No. 17/45, Armament Res. Dept., British M.O.S., Sept. 1945.

2. Ladenburg, R., Van Voorhis, C. C., and Winckler, J.: Interferometric Study of Supersonic Phenomena. Part I: A Supersonic Air Jet at 60 lb/in^2 Tank Pressure. NAVORD Rep. No. 69-46, Bur. Ord., Navy Dept., April 17, 1946.

3. Busemann, Adolf: A Review of Analytical Methods for the Treatment of Flow with Detached Shocks. NACA TN 1858, 1949.

4. Moeckel, W. E., and Connors, J. F.: Charts for the Determination of Supersonic Air Flow against Inclined Planes and Axially Symmetric Cones. NACA TN 1373, 1947.

5. Liepmann, Hans Wolfgang, Askenas, Harry, and Cole, Julian D.: Experiments in Transonic Flow. Tech. Rep. No. 5667, Air Materiel Command, U.S. Air Forces, Feb. 19, 1948. (Prepared by C.I.T., June 1947, under AAF Contract No. W33-038ac-1717 (11592).)

6. Laitone, Edmund V., and Pardee, Otway O'M.: Location of Detached Shock Wave in Front of a Body Moving at Supersonic Speeds. NACA RM A7B10, 1947.

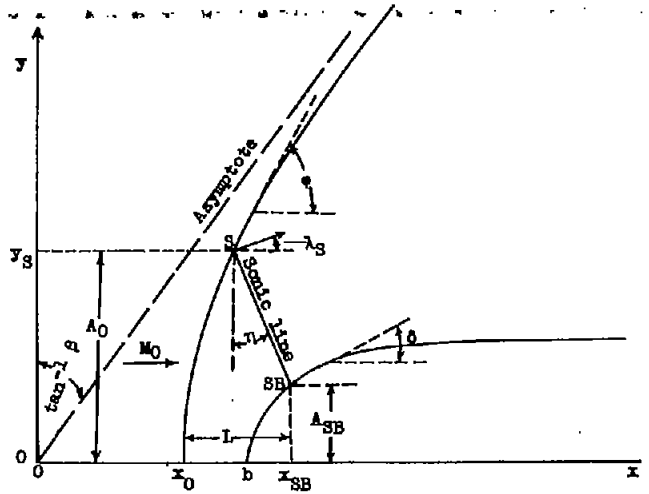

Figure 1. - Representation of flow with detached shock wave and notation used in analysis.

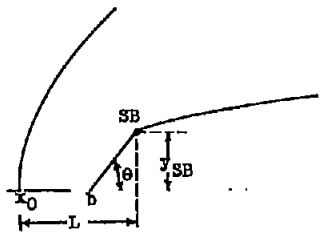

(a) Well-defined shoulders (plane or axially symmetric).

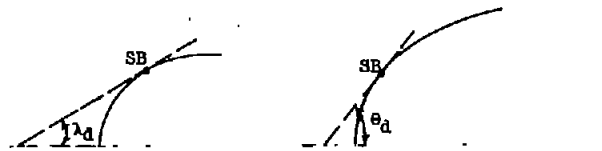

(b) Gradually-curved bodies.

NACA

Figure 2. - Approximate location of body sonic point.

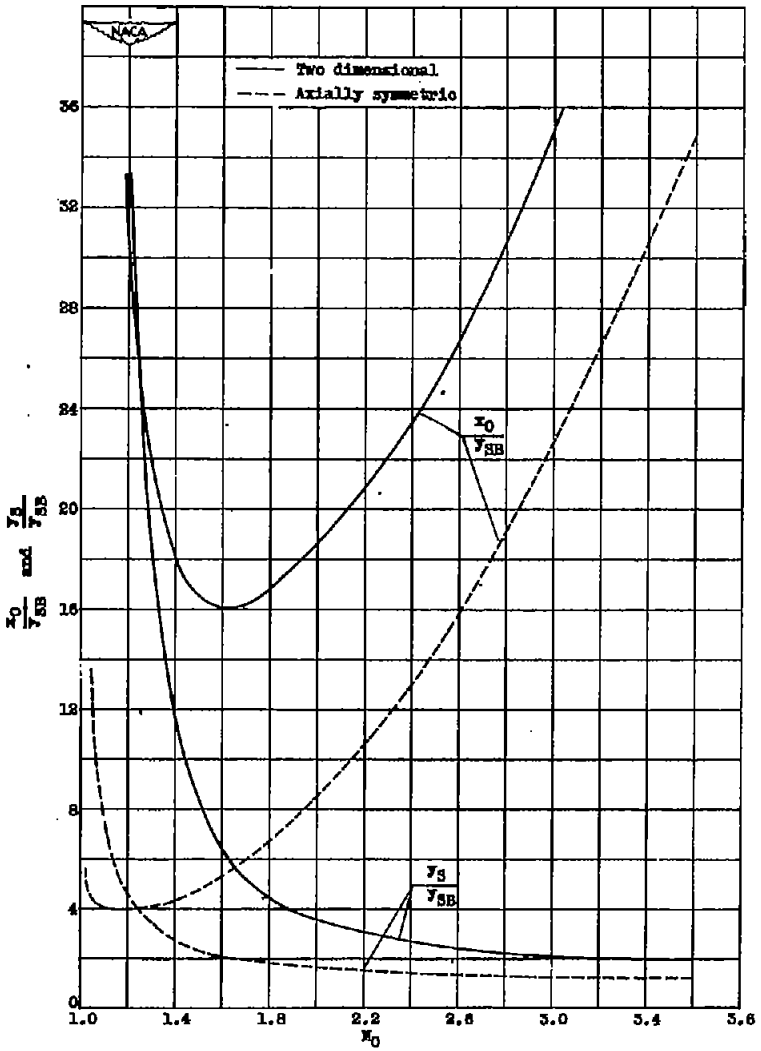

Figure 3. - Parameters for determining shock form and location (continuity method).

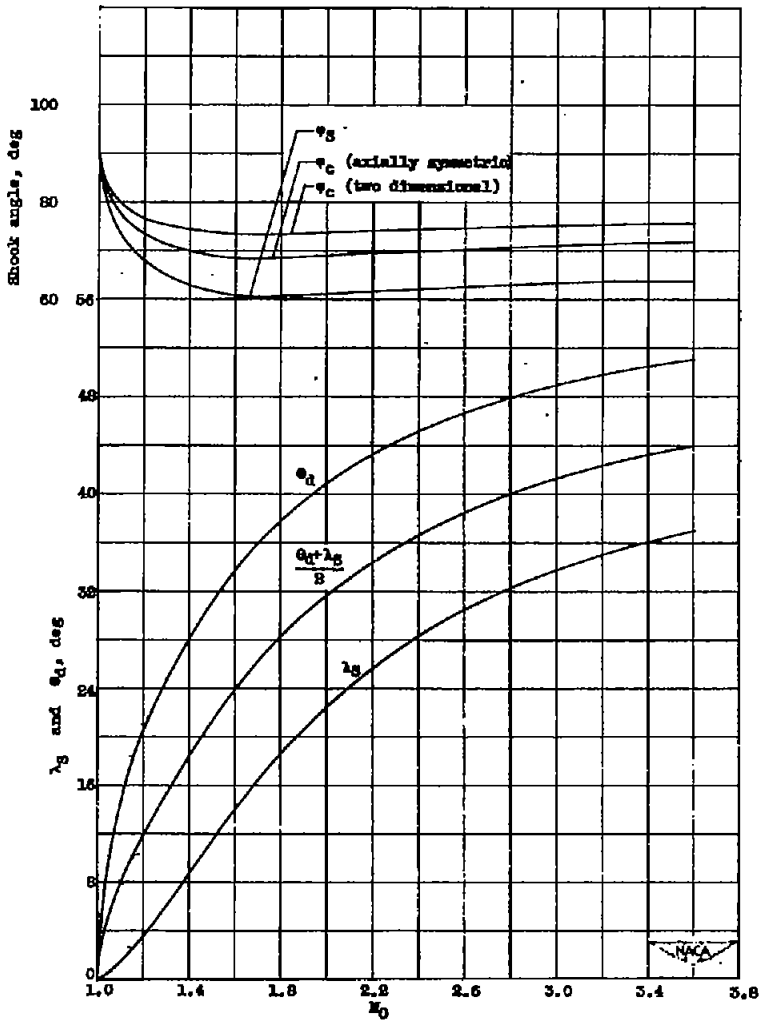

Figure 4. - Variation with Mach number of several angles used in analysis.

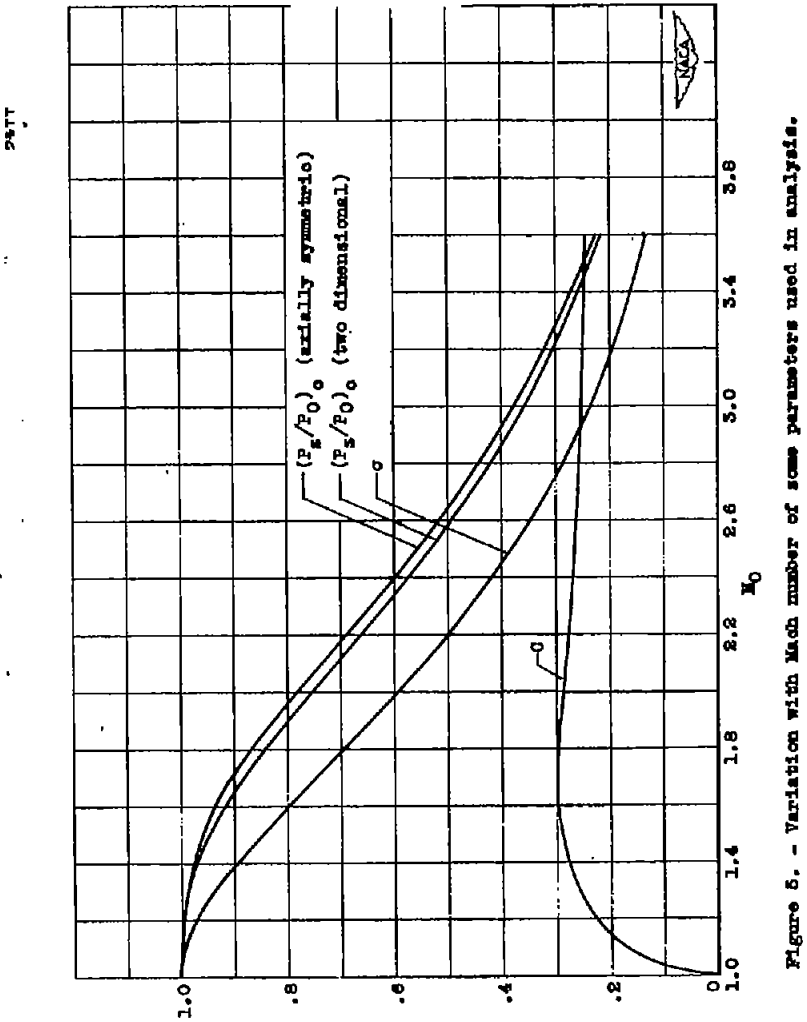

Figure 5. - Variation with Mach number of some parameters used in analysis.

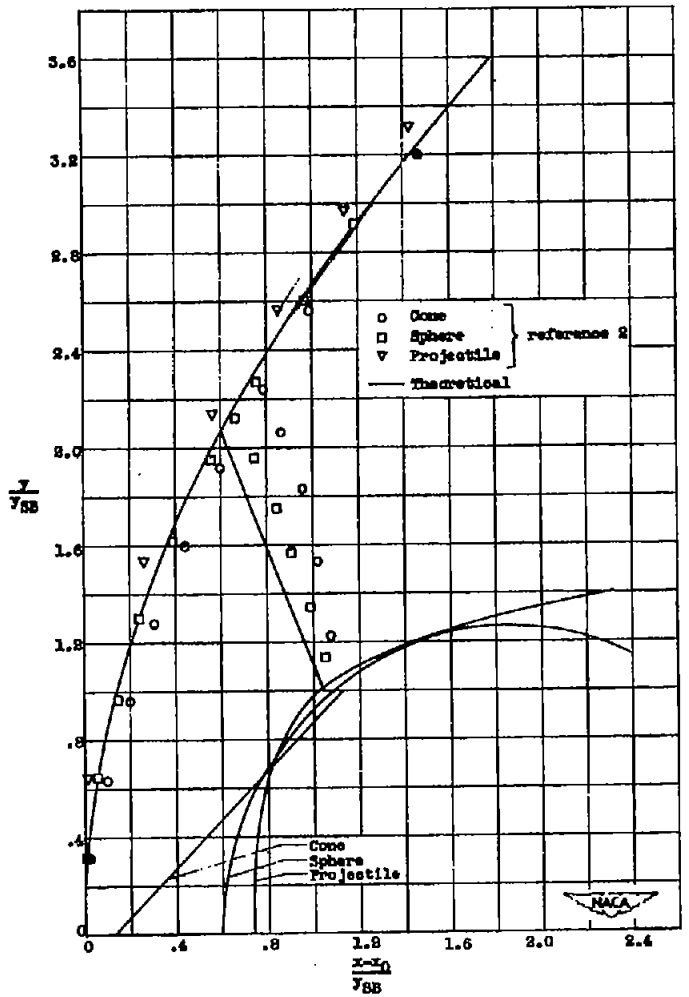

Figure 6. - Comparison of theoretical and experimental shock form, shock location, and sonic line. $M_0 = 1.7$; axially symmetric bodies.

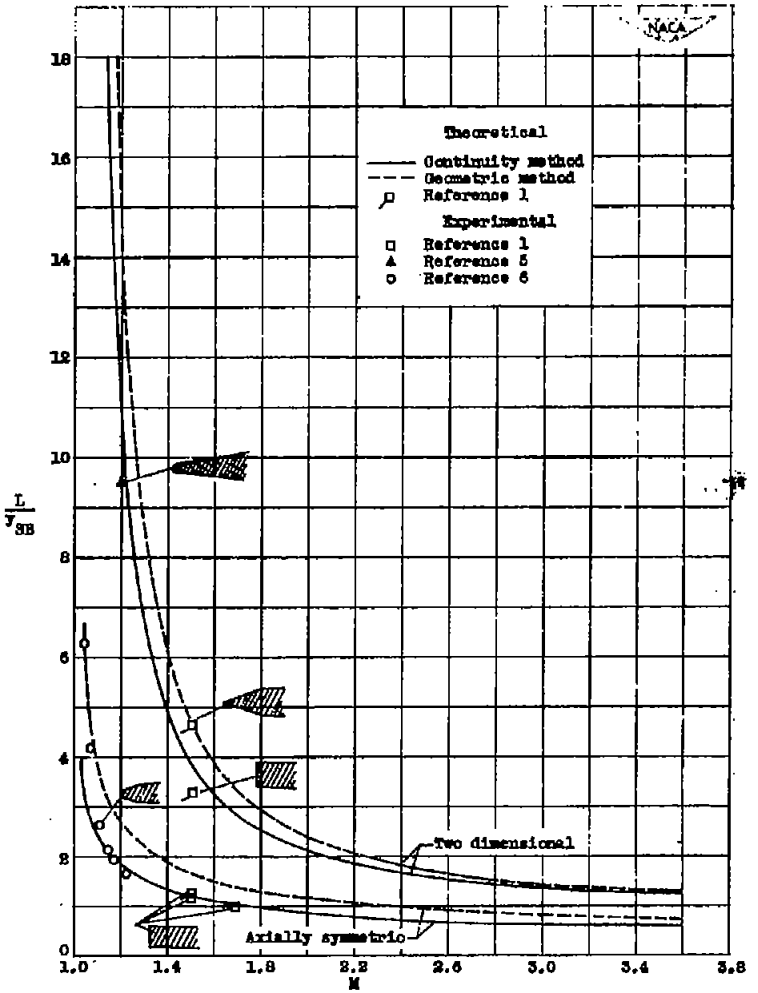

Figure 7. - Theoretical and experimental shock location.

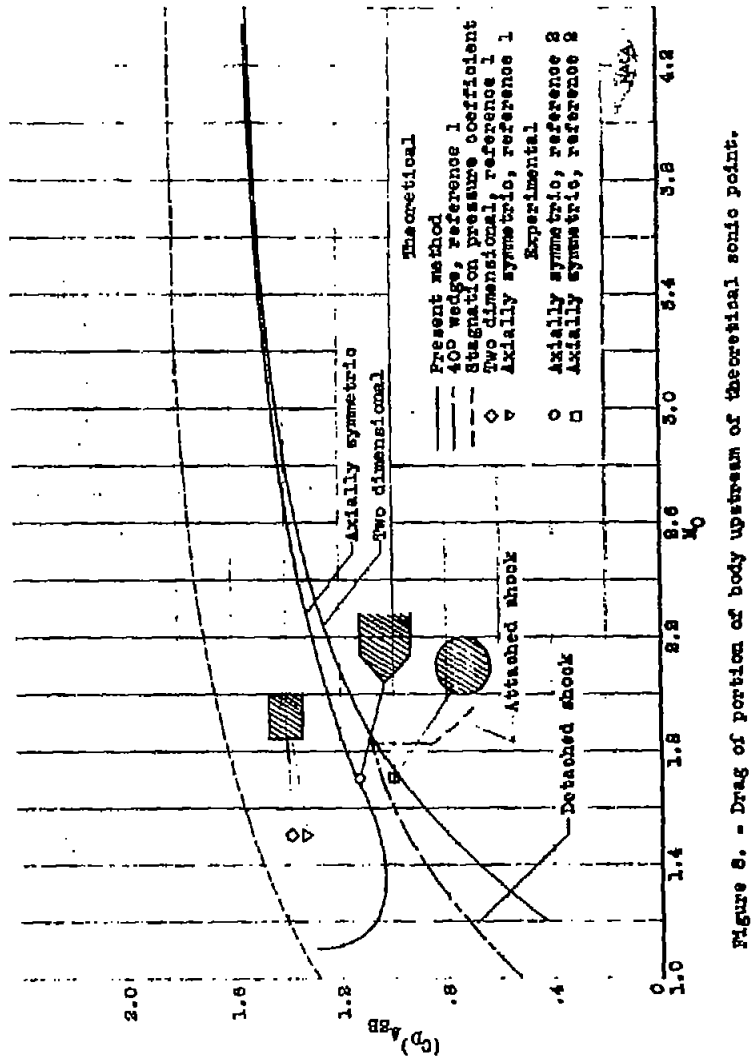

Figure 8. - Drag of portion of body upstream of theoretical sonic point.

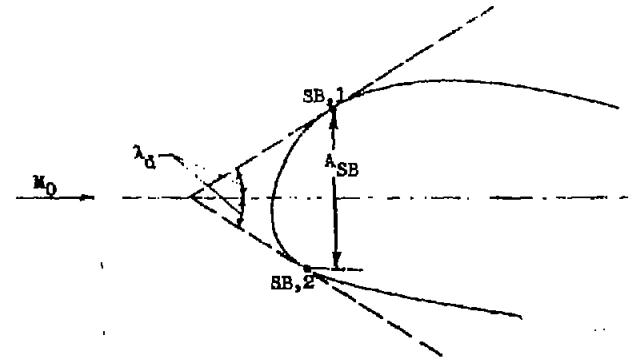

Figure 9. - Determination of sonic points for plane unsymmetric bodies at angle of attack.

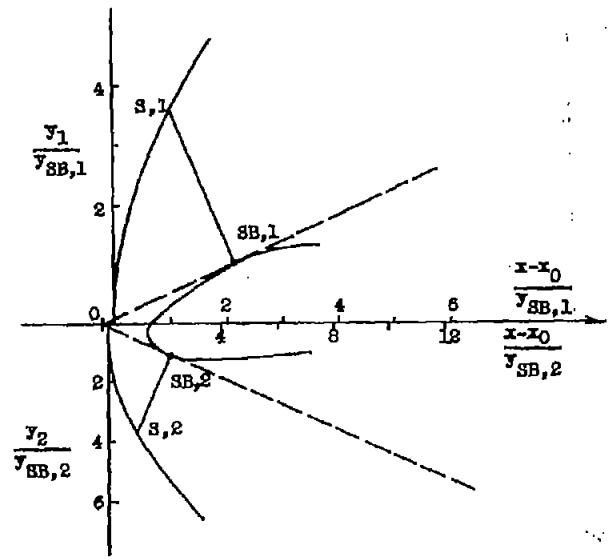

Figure 10. - Predicted relation between detached shock and body sonic points for two-dimensional body when $y_{SB,2} = 0.5y_{SB,1}$, $M_0 = 2.0$.

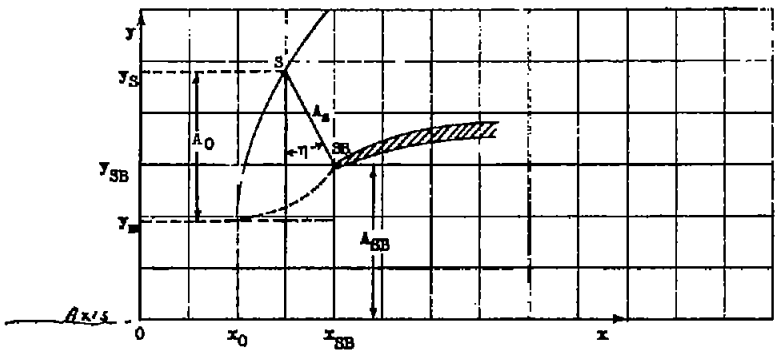

Figure 11. - Simplified picture used for analysis of flow past supersonic inlets with spillage.

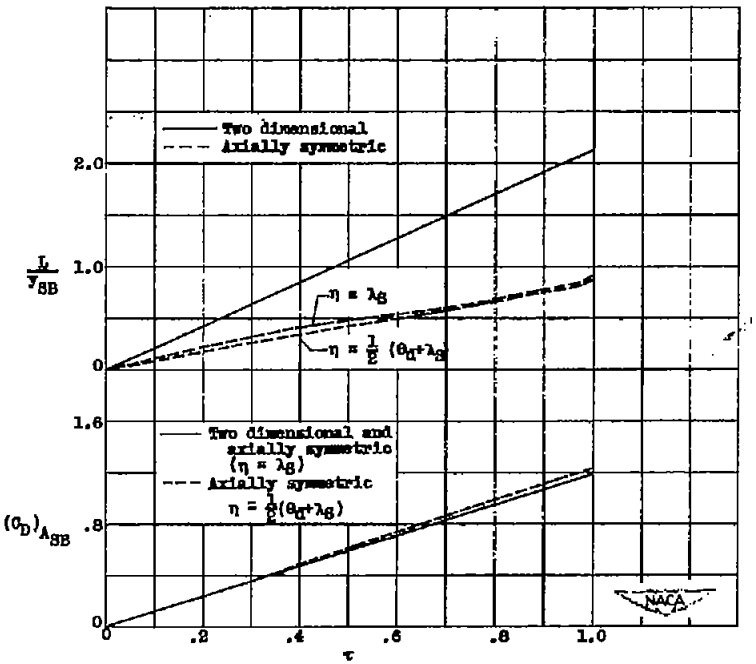

Figure 12. - Shock location and drag as function of spillage. $M_0 = 2.0$.